MIXED CONVECTION IN VERTICAL CONCENTRIC CYLINDERS

Márcio Antonio Bazani
Departamento de Engenharia Mecânica, Universidade Estadual Paulista, Avenida Brasil, 56, 15385-000, Ilha Solteira S.P., Brazil
bazani@dem.feis.unesp.br

Carlos A. C. Altemani
Departamento de Energia, Faculdade de Engenharia Mecânica, Unicamp, C.P. 6122, CEP:13083-970, Campinas S.P., Brazil
altemani@fem.unicamp.br

Abstract. *A numerical and experimental study of the mixed convection in an open annular enclosure was performed under steady state conditions and laminar regime. The enclosure was made from two concentric cylinders, with an annular space for an airflow. The airflow was forced radially into the base of the enclosure, was deflected upward by the inner cylinder and exited the enclosure through the upper annular section. The inner cylindrical wall was isothermal and both the outer cylindrical wall and the base of the enclosure were thermally insulated. The experimental tests comprised three distinct heights for the inflow of air and two diameters of the outer cylindrical wall of the enclosure, for a range of the Reynolds and the Rayleigh numbers. A numerical simulation of the experimental tests was performed from solution of the conservation equations. The simulated values of a Nusselt number defined for the enclosure were in better agrrement with the experimental values for the smaller diameter of the outer cylindrical surface.*

Keywords*: mixed convection, Reynolds, Rayleigh, Nussselt*

1. Introduction

The heat transfer in enclosures has been studied for a variety of engineering application. Results have been presented in research surveys (Afrid and Zebib, 1989, Chang and Chang, 1996, Hashimoto et al., 1990, Hayes, 1990,) and it has become a main topic in convective heat transfer textbooks (Heckel, 1989, Manole and Lage, 1993, Marner and McMillan, 1970, Muralidhar, 1989, Nagendra, 1970, Rogers and Yao, 1989). Usually the enclosures are closed and natural convection is the single heat transfer mechanism. There are however several applications in electric transformer design, heat exchange, nucleate reactor, turbomachines and electronic machines thermal control, where open cavities are employed. In any applications which net power to force fluid flow can be small, as electronic machines cooled, the flow is laminar. So that, the forced convection can suffer a free convection influence and convective heat transfer occurs by combined convection conditions. This work studies the airflow problem into open vertical annular cavity, where cavity inner cylindrical wall is maintained at practically uniform temperature, while the bottom and outer cylindrical wall are isolated thermally. The main convective heat transfer occurs between the airflow and the inner cylindrical surface.

2. Analysis

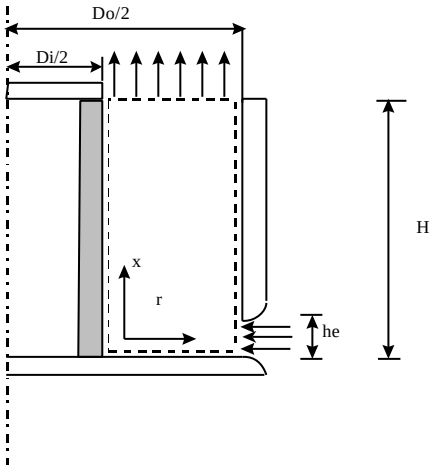

Figure 1 - Domain configuration and notation

The conservation equation of mass, momentum and energy, as well as their boundary conditions, will be expressed for the system indicated in Fig.1. Due to the airflow forced radially into the base of the enclosure, the mixed convection will be considered in the analysis. It is assumed that the flow is laminar and occurs under steady state conditions. The mathematical model was done in cylindrical geometry, involving the continuity, momentum and energy equations and their boundary conditions, into region of fluid flow. Dimensionless equations were used to control the solution. Steady state flow, radial and axial heat transfer, negligible viscous dissipation and axisymmetric heat transfer. The governing equations are given by:

$$\frac{1}{r}\frac{\partial}{\partial r}(r \cdot v) + \frac{\partial u}{\partial x} = 0 \tag{2.1}$$

$$r\left(\mathrm{v}\frac{\partial \mathrm{v}}{\partial \mathrm{r}} + \mathrm{u}\frac{\partial \mathrm{v}}{\partial \mathrm{x}}\right) = -\frac{\partial \mathrm{p}}{\partial \mathrm{r}} + \mu\left[\frac{\partial}{\partial \mathrm{r}}\left(\frac{1}{\mathrm{r}}\frac{\partial}{\partial \mathrm{r}}(\mathrm{r} \cdot \mathrm{v})\right) + \frac{\partial^2 \mathrm{v}}{\partial \mathrm{x}^2}\right] \tag{2.2}$$

The natural convection will be treated via the Boussinesq approximation (Altemani and Chaves, 1989), i.e., density variations are accounted for only when they contribute to buoyancy forces. In this problem, the buoyancy term is obtained from the x momentum equation terms representing the pressure and body forces:

$$-\frac{\partial p}{\partial x} - rg \tag{2.3}$$

The density is related to temperature according to the Boussinesq approximation:

$$r = r_{in} - r_{in} gb\left(T - T_{in}\right) \tag{2.4}$$

In (2.4) T_{in} indicates the temperature of the fluid inlet at annular region and ρ_{in} the corresponding density. The pressure is now expressed in terms of a modified pressure defined as:

$$\overset{*}{p} = p + r_{in} gx \tag{2.5}$$

With (2.4) and (2.5), the equation (2.3) can be expressed by:

$$-\frac{\partial \overset{*}{p}}{\partial x} + r_{in} gb\left(T - T_{in}\right) \tag{2.6}$$

The second term in this equation relates the buoyancy forces to temperature differences ($T-T_{in}$). From this formulation, the density will be assumed constant and equal to ρ_{in} in all the equations, so that the subscript in may be deleted. The momentum equation in the axial direction is given by:

$$r\left(u\frac{\partial u}{\partial x} + v\frac{\partial u}{\partial r}\right) = -\frac{\partial \overset{*}{p}}{\partial x} + rgb\left(T - Tin\right) + m\left[\frac{1}{r}\frac{\partial}{\partial r}\left(r\frac{\partial u}{\partial r}\right) + \frac{\partial^2 u}{\partial x^2}\right] \tag{2.7}$$

The energy equation is given by:

$$r \cdot c_p \cdot \left(v\frac{\partial T}{\partial r} + u\frac{\partial T}{\partial x}\right) = k\left[\frac{1}{r}\frac{\partial}{\partial r}\left(r\frac{\partial T}{\partial r}\right) + \frac{\partial^2 T}{\partial x^2}\right] \tag{2.8}$$

In order to obtain the conservation equations in dimensionless form, was considered a reference velocity $\mathrm{v}_0 = \sqrt{g \cdot b \cdot \left(T_w - T_{in}\right) \cdot H}$, to the velocities components where $\left(T_w - T_{in}\right)$ corresponds to difference between wall and inlet temperatures. The following variables were defined:

$$X = \frac{x}{H};\ R = \frac{r}{H};\ U = \frac{u}{v_0};\ V = \frac{v}{v_0};\ P = \frac{\overset{\bullet}{p}}{r \cdot v_0^{\,2}};\ q = \frac{T - T_{in}}{T_w - T_{in}};\ \mathrm{Pr} = \frac{u}{a};\ Ra = \frac{\left[g \cdot b \cdot \left(T_w - T_{in}\right)\right] \cdot H}{u \cdot a};\ \mathrm{Re} = \frac{4\overset{\bullet}{m}}{p\left(D_o + D_i\right)m}$$

The equations expressing continuity, r and x momentum and energy the become:

$$\frac{1}{R}\frac{\P}{\P R}(R\cdot V)+\frac{\P U}{\P X}=0 \tag{2. 9}$$

$$U\frac{\P V}{\P X}+V\frac{\P V}{\P R}=-\frac{\P P}{\P R}+\sqrt{\frac{\Pr}{Ra}}\left[\frac{\P}{\P R}\left(\frac{1}{R}\frac{\P(RV)}{\P R}\right)+\frac{\P^2 V}{\P X^2}\right] \tag{2.10}$$

$$U\frac{\P U}{\P X}+V\frac{\P U}{\P R}=-\frac{\P P}{\P X}+q+\sqrt{\frac{\Pr}{Ra}}\left[\frac{1}{R}\frac{\P}{\P R}\left(R\frac{\P U}{\P R}\right)+\frac{\P^2 U}{\P X^2}\right] \tag{2.11}$$

$$V\frac{\P q}{\P R}+U\frac{\P q}{\P X}=\frac{1}{\sqrt{\Pr\cdot Ra}}\left[\frac{1}{R}\frac{\P}{\P R}\left(R\frac{\P q}{\P R}\right)+\frac{\P^2 q}{\P X^2}\right] \tag{2.12}$$

The velocity components are null at inner cylindrical wall and the thermal boundary conditions comprise a uniform temperature at the wall, thus θ = 1.0. Expressed in dimensionless terms, the boundary conditions become:

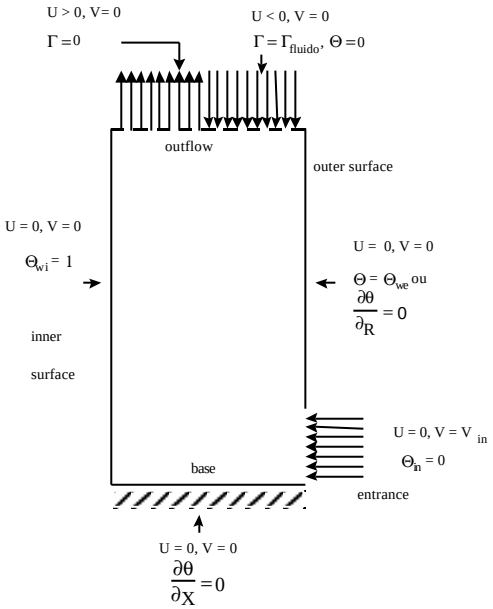

Figure 2 – Boundary conditions

At entrance of the cavity, were considered U=0, V=(v_{in}/v_o) and θ=0. At outer cylindrical wall, due to surface impermeability U e V are null, and for energy equations were assumed two hypothesis. The first hypothesis is adiabatic wall and the second hypothesis is uniform temperature at wall. The outflow boundary of the open cavity, at X=1, is just a virtual boundary defining the calculation domain. In order to obtain a solution, two conditions must be no back flow of fluid and second, there must be no diffusion from outside into the calculation domain. The first condition was verified checking the velocity profiles of each result obtained and discarding those results when a back flow was observed. The second was satisfied imposing artificially negligible partial derivatives of θ and U in the vertical direction at the outflow boundary. The velocity component V was corrected at the outflow boundary in order to satisfy the continuity equation in the whole domain. The differential equations (2.9) to (2.11) together with their boundary conditions, comprise a coupled system involving the four variables U, V, P and θ. The equations were discretized using the control volume formulation described in (Patankar, 1981) and the solution was obtained employing the SIMPLE scheme. The convergence of the results was accepted when the relative change of the dependent variables was under 10^{-7}. An investigation of the number of grid points will be presented with the results.

3. Experimental Analysis

The experimental data were obtained changing the air flow, the dissipated electric power and the geometry of the annular duct. The results were reduced in function of the Nusselt, Reynolds and Grashoff numbers. The enclosure was made from two concentric cylinders, with an annular space for an airflow. The airflow was forced radially into the base of the enclosure, was deflected upward by the inner cylinder and exited the enclosure through the upper annular section. The inner cylindrical was composed by aluminum thick wall, with a electric resistance, to provide constant wall temperature. The outer cylindrical was involved by fiberglass insulation. The total set of experimental measured was done varying two geometric parameters: outer diameter D_e and the height h_e of the air entrance. Besides, also were varying the dissipated electric power in the cylinder and the air flow rate. The following configurations were tested:- Configuration 1: D_e=9.75 cm e h_e = 6.2 cm;- Configuration 2: D_e=9.75 cm e h_e = 3.2 cm;- Configuration 3: D_e=9.75 cm e h_e = 1.2 cm;- Configuration 4: D_e=7.1 cm e h_e = 6.2 cm;- Configuration 5: D_e=7.1 cm e h_e = 3.2 cm;- Configuration 6: D_e=7.1 cm e h_e = 1.2 cm.

4. Results and Discussions

The simulations were based in the geometric parameters of the experimental cavity. The measured values at lab of Reynolds and Rayleigh numbers were used in the simulations. The fluid properties (air) were evaluated in the mean temperature between T_w e T_{in}. The Reynolds numbers were in the range of 100 and 600. The measured were done, in each value Re, in two levels of Rayleigh numbers, to investigate the influence of the free convection. A refinement study was realized to define the grid in the simulations. In the first set, was considered Re=100.6 while Ra=5.88e6. In the second set, was considered Re=588,26 and Ra=5.93e6. The simulations were done for several distinct grids, as showed fig. 3. The coarse grid had 16 x 30 control volumes and the finest grid had 60 x 30. The grid used in the numerical simulation was 55 x 30. Increasing the number of grid points from 1650 to 1800 would change the average Nusselt number by approximately 1%. The influence of the Ra for several Reynold numbers is showed in the fig. 4, with air properties to 300 K. The free convection does not change the results of the forced convection , that is characterized by Re. Due to experimental limitation was not possible to realize measurements with higher values of Ra. At simulation level, would be possible to consider higher values of Ra, but the steady state could be not validate and thus were not considered. The simulation results showed in the fig. 5 were obtained considering adiabatic external cylindrical wall. The same results were obtained considering isothermal wall θ_{we} = 0.1. This value corresponds to temperature higher than those measured in the experimental tests, warmed by radiation effects. The consideration as adiabatic wall has not affected the Num_2 results. The experimental and simulation results of the series 1 are showed in the figure 5.3. The differences between the experimental values and the simulation values are lower than 10%. This difference is caused by experimental uncertainties and also when were used higher diameters and higher heights of air flow entrance.

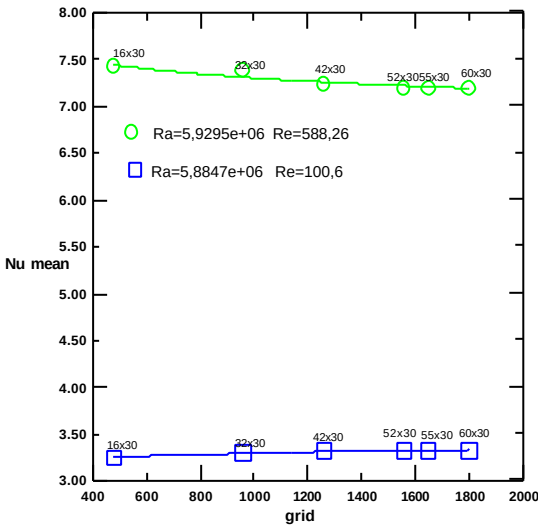

Figure 3 - Nu mean x grid

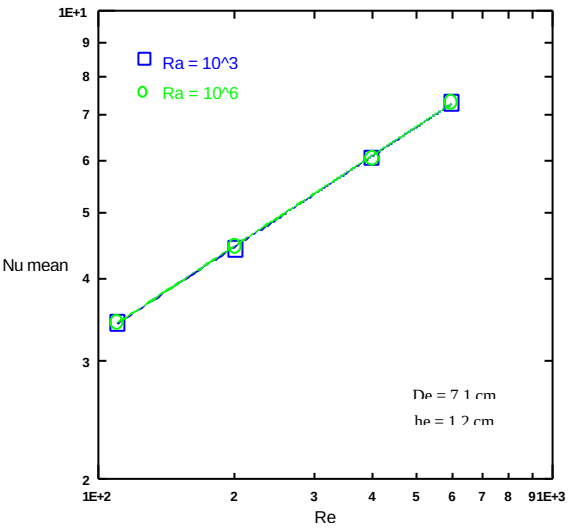

Figure 4 - Nu mean x Re

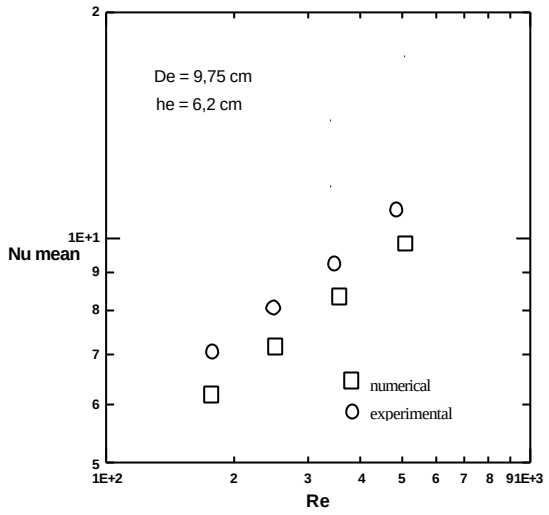

Figure 5 - Num$_D$ x Re (series 1)

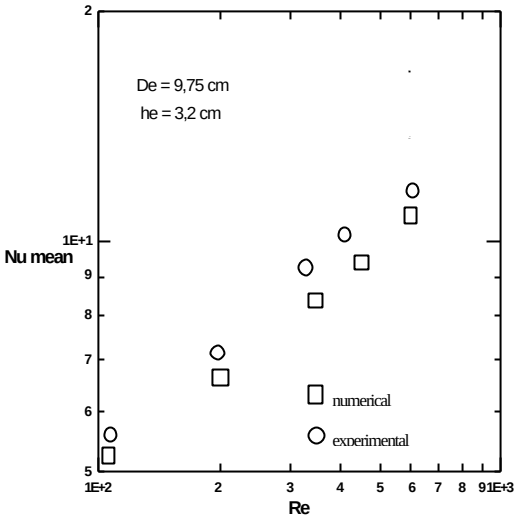

Figure 6 - Num$_D$ x Re (series 4)

The experimental and simulation results of the series 4 are showed in the fig. 6. The differences between experimental values and simulation values for mean Nusselt number are lower than 10%. These differences are lower than series 1, due to lower height of air flow entrance (h_e = 3,2 cm). In the fig. 5 and 6, the experimental values of mean Nusselt number were higher than the simulation values. The simulations were done with hypothesis of steady state. Can be considered that in this case, the air flow in the cavity entrance has a characteristic of transition or turbulent regime, causing a increased in the experimental mean Nusselt.

The experimental and simulation results of the series 5 are showed in the fig. 7. This series is interesting, because the diameter is higher (D_e = 9,75 cm), however the height of the air flow entrance diminished (h_e = 1,2 cm). The differences between the experimental values and simulation values for mean Nusselt number are approximately 10% (experimental uncertainties). Apparently, the perturbations were maintained into a tolerable level for steady state, due to decreased of the height of air flow entrance.

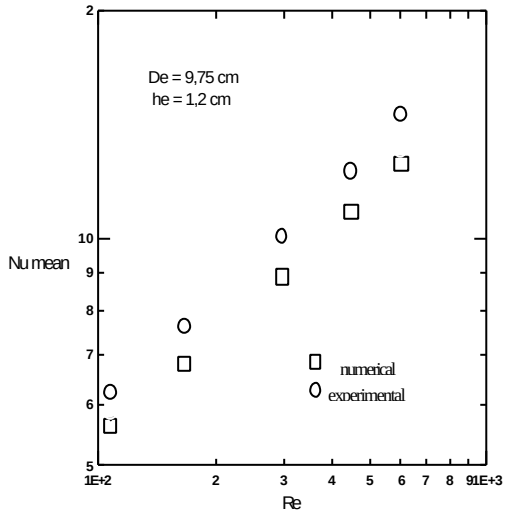

Figure 7 - Num$_D$ x Re (series 5)

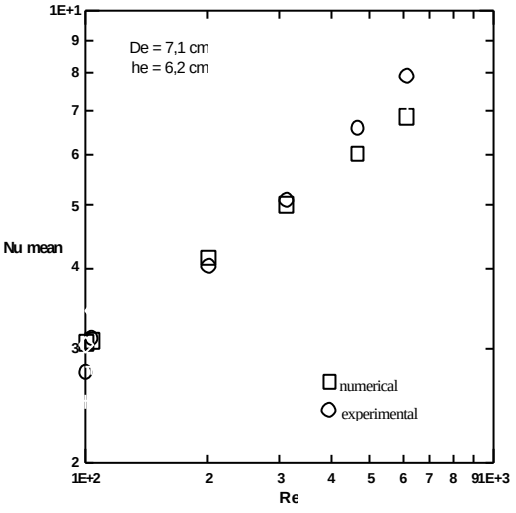

Figure 8 - Num$_D$ x Re (series 2)

The experimental and simulation results of the series 2 are showed in the fig. 8. The differences between experimental and simulation results for mean Nusselt number are into experimental uncertainties. The two curves intercept themselves at Re 200. This decreased in the discrepancies compared with fig. 7 is due to lower diameter of the cavity external wall.

The experimental and simulation results of the series 3 are showed in the fig. 9. The differences between experimental and simulation results for mean Nusselt number are into experimental uncertainties. The two curves intercept themselves at Re 300.

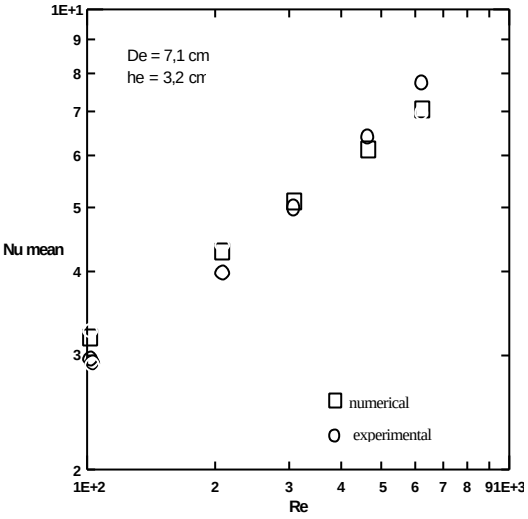

Figure 9 - Num$_2$ x Re (series 3)

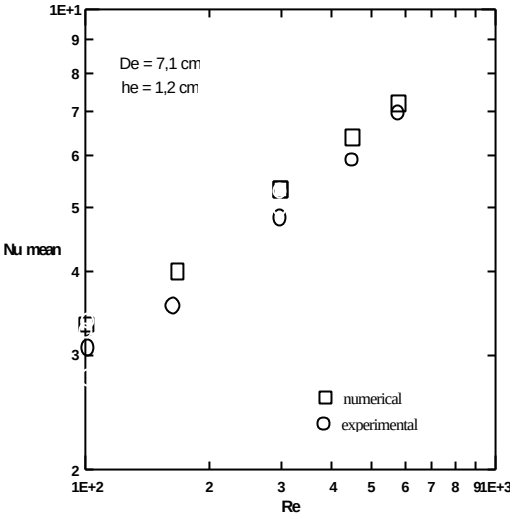

Figure 10 – Num$_2$ x Re (series 6)

The experimental and simulation results of the series 6 are showed in the fig. 10. The differences between experimental and simulation results for mean Nusselt number are into experimental uncertainties. The two curves did not intercept themselves, but were near to Re 600. At simulations, the air flow entered radial into cavity, with uniform velocity, without velocity axial component.

5. Conclusions

The results obtained to indicate into the investigate range of Re, that the influences of natural convection and of the height of air flow entrance can not measured experimental because they are into of measured uncertainties. The higher diameter of cylinder to implicate in higher heat transfer rates by convection for the same Reynolds number, because of the higher air flow rate by annular duct due to increased of the hydraulic diameter. As the air flow rate increases, the mean mixed temperature diminishes, favoring the heat transfer. In the range of Reynolds and Grashoff investigated, in this work, for the same diameter of outer cylinder, the heat transfer into annular duct depends of the Reynolds number. The experimental results of mean Nusselt due to temperature difference (T_w - T_{in}) were reproduced by simulation for lower diameters of the cavity external surface. For the surface with higher external diameter, the simulation with lower height of air entrance presented good concordance with experimental results.

6. Acknowledgements

Special gratitude is given to Carlos A. C. Altemani who helped me in the orientation and writing this work.

7. Nomenclature

A - área total área of heat transfer	[m^2]
c_p – specific heat transfer	[Ws / kgK]
D_h – hydraulic diameter	[m]
D_i – inner diameter of the cylinder	[m]
D_o – outer diameter of the cylinder	[m]
g – gravity acceleration	[m/s^2]
h – convective coefficient of the heat transfer	[W / m^{2O}C]
h_e – height of the air flow entrance	[m]
H – height of the cylinder	[m]
k_f – thermal conductivity of the fluid	[W / m ^{o}C]
m- total mass flow	[kg / s]
Nu – Nusselt number	
p – fluid pressure	[Pa]
p_{atm} – atmospheric pressure	[Pa]
p* - corrected fluid pressure	[Pa]
P – dimensionless corrected fluid pressure	
Pr – Prandtl number	

$\mathbf{q_{conv}}$ – convective heat transfer	[W / m]
r - radial coordinate	[m]
R – dimensionless radial coordinate	
Ra – Rayleigh number	
$\mathbf{Re_{DH}}$ – Reynolds number based at hydraulic diameter	
T – fluid temperature	[K]
$\mathbf{T_{in}}$ – air entrance temperature	[K]
$\mathbf{T_w}$ – outer surface cylindrical of the cavity	[K]
u – axial velocity of the fluid	[m / s]
U – dimensionless axial velocity of the fluid	
v – radial velocity of the fluid	[m/s]
$\mathbf{v_0}$ – reference velocity	[m/s]
V – dimensionless radial velocity of the fluid	
x - axial coordinate	[m]
X - dimensionless axial coordinate	
a – thermal diffusivity	
b_0 – Boussinesq coefficient	[1 / K]
r_e – air density	[kg/ m^3]
q – dimensionless temperature	
m – kinematics viscosity	[kg/ m s]
n – dynamic viscosity	[m^2 / s]

4. References

Afrid, M, Zebib; A Natural convection air cooling of heated components mounted on a vertical wall. *Numerical Heat Transfer*, v.15, part A, p.243-259, 1989.

Altemani, C. A, Chaves; C. A. Convective cooling of a semiporous open cavity. *ASME Heat Transfer in Eletronics*, HTD - v.111, p. 149-154, 1989.

Chang, W. J., Chang, W. L. Mixed convection in a vertical parallel - plate channel partially filled with porous media of high permeability. *International Journal Heat Transfer*, v.31, n 7, p.1331-1342, 1996.

Hashimoto, K., Akino, N., Kawamura, H.. Simulation of mixed convection heat transfer at the wall of a packed bed. *International Journal of Heat Transfer*, v.33, n 1, p.79-90, january 1990.

Hayes, R. E. Simulation of mixed convection heat transfer at the wall of a packed bed. *Numerical Heat Transfer*, v.17, part A, p.217-230, 1990.

Heckel, J. J., Chen, T. S., Armaly, B. F. Mixed convection along slender vertical cylinders with variable surface temperature. *International Journal Heat Mass Transfer*, v.32, n 8, p.1431-1442, 1989.

Manole, D.M., Lage, J. L.. Nonuniform grid accuracy test applied to the natural - convection flow within a porous medium cavity. *Numerical Heat Transfer*, v.23, part B, p.351-368, 1993.

Marner, W.J., Mcmillan, H. K. Combined free and forced laminar convection in a vertical tube with constant wall temperature. *Journal of Heat Transfer*, p.559-562, august 1970.

Muralidhar, K. Mixed convection flow in a saturated porous annulus, *International Journal Heat Mass Transfer*, v.32, n 5, p.881-888, 1989.

Nagendra, H.R., Tirunarayanan, M. A., Ramachandran, A. Laminar free convection from vertical cylinders with uniform heat flux. *Journal of Heat Transfer*, p.191-194, february 1970.

Patankar, S. V.. A calculation procedure for two - dimensional elliptic situations. *Numerical Heat Transfer*, v.4, n.6, p.409-425, 1981.

Rogers, B. B., Yao, L. S. Mixed convection in an annulus of large aspect ratio. *Journal of Heat Transfer*, v.111, p.683-689, august 1989.